Mixed-Mode Effect on Motor Common Mode Current

Vefa Karakasli and Gerd Griepentrog
Institute of Power Electronics and Control of Drives
Technical University Darmstadt
Darmstadt, Germany
vefa.karakasli@lea.tu-darmstadt.de, gerd.griepentrog@lea.tu-darmstadt.de

Junsheng Wei and Danil Drozhzhin
Research and Technology Center
ZF Friedrichshafen AG
Friedrichshafen, Germany
junsheng.wei@zf.com, danil.drozhzhin@zf.com

Abstract—**This paper presents the mixed-mode effect on motor common mode current (CMC) in an adjustable speed drive (ASD). It is expected that the motor CMC is lower than inverter output CMC. However, the measurement result of the ASD shows that the AC motor input CMC is higher than the inverter output CMC in a frequency range. By using a mixed-mode (MM) 6-port networks, it is proven that the AC motor input CMC is higher due to an MM CMC which is generated from differential mode current.**

Index Terms—**AC drive, CM, frequency domain model, mixed-mode, six-port network.**

I. Introduction

Wide-bandgap (WBG) semiconductors, such as silicon carbide (SiC), has a trending to be used for application of adjustable speed drives (ASDs), since they have great operational advantages such as switch higher current and voltage, faster switching and higher operational temperature [1], [2]. This allows to the designer to increase the frequency of power converter to achieve a lower size. Meanwhile, the fast rise and fall time transient of SiC semiconductors cause electromagnetic interference (EMI) challenges which are EMI effect to the neighbour devices, higher bearing current and deterioration of motor winding insulations [3], [4]. There are some international EMC standards which define limitations to minimize EMI problems. Therefore, it is important to predict the generated EMI noise accurately and use a suitable solution to minimize the aforementioned problem.

In a simplified equivalent common mode (CM) circuit of the ASDs, the common mode current (CMC) is induced by the high switching patterns ($\frac{\mathrm{d}v}{\mathrm{d}t}$) between the converter and ground terminals [5]. The CMC at AC side flows through the parasitic capacitances of inverter, EMI filter, 3-phase shielded cable and motor to ground, as shown in Fig. 1. Considering the simplified CM circuit, the summation of cable and motor CMCs are equal to filter output CMC as expressed in (1):

$$I_{\mathrm{CM_o}} = I_{\mathrm{CM_{cab1}}} + I_{\mathrm{CM_{cab2}}} + I_{\mathrm{CM_{mot}}}. \tag{1}$$

However, the measurements show that $I_{\mathrm{CM_{mot}}}$ is higher than $I_{\mathrm{CM_o}}$ in the frequency range (0.5-25MHz), as shown in Fig. 2. The main reasons for this phenomenon are the coupling between CM and differential mode (DM) caused by asymmetry of the three-phase system and non-linear operation
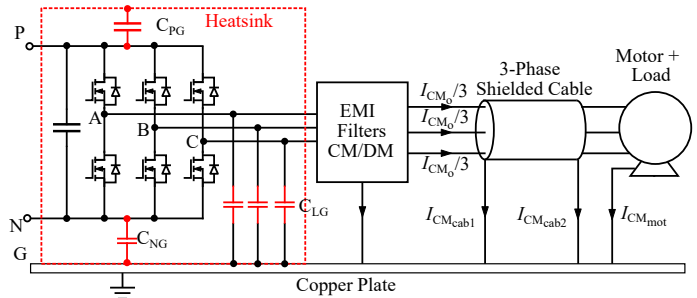
Fig. 1. The detailed model of AC side of ASD.
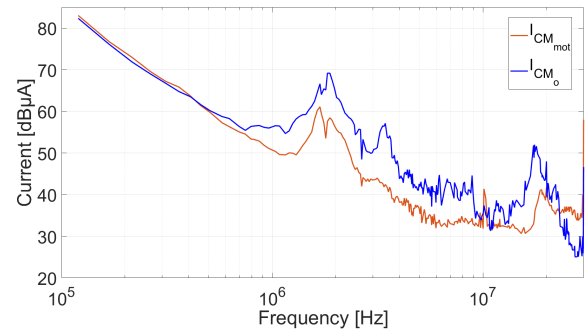
Fig. 2. Output side CMC measurements.

of inverter [6], [7]. This phenomenon is called mixed-mode (MM) effect. In this paper, the MM in motor CMC will be considered.

II. Model Description and Results for Motor Common Mode Current

A 6-port MM behavioral frequency domain model is used to model the effect of DM on CM which is explained in deeply in [6]. Here, the DC side of ASD, which influences pure CMC and induced CMC due to MM, is also added as given in Fig. 3. The CM voltage in (2) is coupled with two DM voltages in (3) by 6-port MM impedance ($\mathbf{Z}_{\mathrm{MM}}$) which is obtained 6-port single-ended impedance ($\mathbf{Z}_{\mathrm{SE}}$) measurement by using the transformation matrix in (4):

$$U_{\mathrm{CM}} = \frac{U_{\mathrm{A}} + U_{\mathrm{B}} + U_{\mathrm{C}}}{3}, \tag{2}$$

$$U_{\text{DM}_1} = U_{\text{A}} - U_{\text{B}}, \tag{3}$$
$$U_{\text{DM}_2} = U_{\text{B}} - U_{\text{C}},$$

$$\mathbf{Z}_{\text{MM}} = \mathbf{T}\mathbf{Z}_{\text{SE}}\mathbf{T}^{-1}. \tag{4}$$

The DC side equivalent circuit of CM (Z_{CM_i}) is calculated from the impedance parameter analysis of terminated 2-port based on Fig. 3 (a). The 2-port input CM and two DM chain parameters matrices which are calculated from (5) and (6) are coupled to get the input 6-port chain parameters matrix ($\mathbf{ABCD}_{\text{in}}$). 6-port $\mathbf{Z}_{\text{MM}}$ of EMI filter, AC cable and motor are transferred to 6-port chain parameters for cascade connection of system. Then, all 6-port chain matrices, which are $\mathbf{ABCD}_{\text{in}}$, $\mathbf{ABCD}_{\text{cab}}$, $\mathbf{ABCD}_{\text{fil}}$ and $\mathbf{ABCD}_{\text{mot}}$, are cascade connected to obtain a total 6-port system chain matrix ($\mathbf{ABCD}_{\text{tot}}$).

$$\begin{bmatrix} A_{\text{CM}_{\text{in}}} & B_{\text{CM}_{\text{in}}} \\ C_{\text{CM}_{\text{in}}} & D_{\text{CM}_{\text{in}}} \end{bmatrix} = \begin{bmatrix} 1 + Z_{\text{CM}_i}Y_{\text{CM}_i} & Z_{\text{CM}_i} \\ Y_{\text{CM}_i} & 1 \end{bmatrix}, \tag{5}$$

$$\begin{bmatrix} A_{\text{DM}_{k,\text{in}}} & B_{\text{DM}_{k,\text{in}}} \\ C_{\text{DM}_{k,\text{in}}} & D_{\text{DM}_{k,\text{in}}} \end{bmatrix} = \begin{bmatrix} 1 & Z_{\text{DM}_{k,\text{in}}} \\ 0 & 1 \end{bmatrix} \qquad k = 1, 2. \tag{6}$$

In order to find the input currents and motor output currents, $\mathbf{ABCD}_{\text{tot}}$ is transferred to an admittance matrix $\mathbf{Y}_{\text{tot}}$ and admittance matrix equation is used as given (7). $\mathbf{ABCD}_{\text{in}}$, $\mathbf{ABCD}_{\text{cab}}$ and $\mathbf{ABCD}_{\text{fil}}$ are cascade connected to calculate the motor input current from the inverse chain parameters equation in (8):

$$\begin{bmatrix} I_{\text{CM}_u} \\ I_{\text{DM}_{1u}} \\ I_{\text{DM}_{2u}} \\ I_{\text{DM}_{3\text{mot,o}}} \\ I_{\text{DM}_{1\text{mot,o}}} \\ I_{\text{DM}_{2\text{mot,o}}} \end{bmatrix} = \mathbf{Y}_{\text{tot}} \begin{bmatrix} U_{\text{CM}} \\ U_{\text{DM}_1} \\ U_{\text{DM}_2} \\ 0 \\ 0 \\ 0 \end{bmatrix}, \tag{7}$$

$$\begin{bmatrix} U_{\text{CM}_{\text{mot,i}}} \\ U_{\text{DM}_{1\text{mot,i}}} \\ U_{\text{DM}_{2\text{mot,i}}} \\ I_{\text{CM}_{\text{mot,i}}} \\ I_{\text{DM}_{1\text{mot,i}}} \\ I_{\text{DM}_{2\text{mot,i}}} \end{bmatrix} = \mathbf{ABCD}_{\text{in,cab,fil}}^{-1} \begin{bmatrix} U_{\text{CM}} \\ U_{\text{DM}_1} \\ U_{\text{DM}_2} \\ I_{\text{CM}_u} \\ I_{\text{DM}_{1u}} \\ I_{\text{DM}_{2u}} \end{bmatrix}. \tag{8}$$

The motor input CMC ($I_{\text{CM}_{\text{mot,i}}}$) consists of pure CMC and MM CMC. It is possible to find these two CMCs separately. If U_{CM} is assigned by 0, the MM CMC of motor will be obtained. In case of $U_{\text{DM}_1} = U_{\text{DM}_2} = 0$, the pure CMC of motor is calculated. The simulated CMC of motor is compared with measured result in Fig. 4. It can be observed that the simulated result matches very well with measured results except for the HF resonance peak (18MHz) because of the difficulties of HF impedance prediction. The MM $I_{\text{CM}_{\text{mot,i}}}$ is more dominant than the pure one in 0.55-22MHz frequency range. This is reason why $I_{\text{CM}_{\text{mot,i}}}$ is higher then I_{CM_o}.

III. CONCLUSION

In this paper, a fast prediction method is proposed to model the effect of MM current on motor CMC. The simulation results are also proven by measurement results. This research will help ASD designers to take precautions against CMC effect on bearing current and deterioration of motor windings.

(a) Input

(b) Input and output
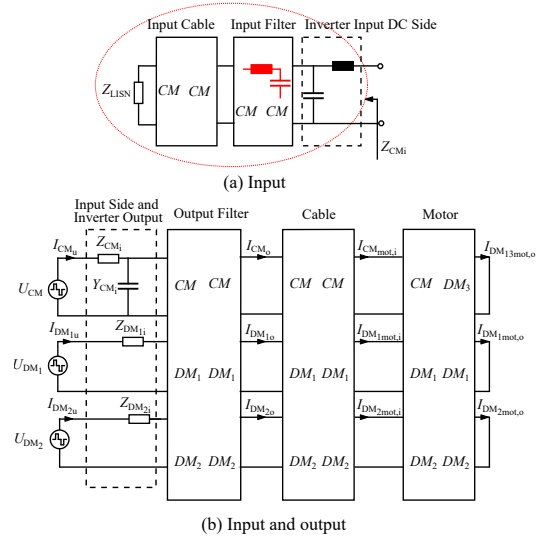
Fig. 3. 6-port MM EMC prediction model.
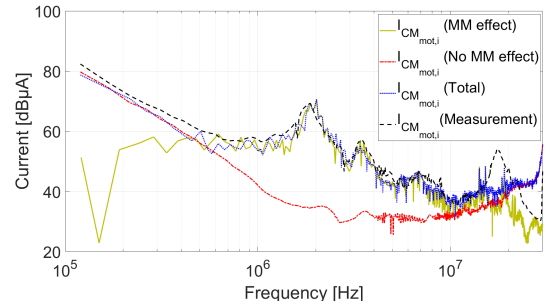
Fig. 4. The simulation result of motor CMC are compared with measurement results.

IV. ACKNOWLEDGMENT

REFERENCES

[1] S. Tanimoto and K. Matsui, "High junction temperature and low parasitic inductance power module technology for compact power conversion systems," IEEE Trans. Electron Devices, vol. 62, no. 2, pp. 258-269, Feb. 2015.

[2] X. Ding, et al., "Analytical and experimental evaluation of SiC-inverter nonlinearities for traction drives used in eletric vehicles," IEEE Trans. Veh. Technol., no. 99, pp. 1, 2017.

[3] G. Vidmar and D. Miljavec, "A Universal High-Frequency Three-Phase Electric-Motor Model Suitable for the Delta- and Star-Winding Connections," IEEE Transactions on Power Electronics, vol. 30, pp. 4365-4376, 2015.

[4] H. Chen, Y. Yan, and H. Zhao, "Extraction of common-mode impedance of an inverter-fed induction motor," IEEE Trans. Electromagn. Compat., vol. 58, no. 2, pp. 599-606, Apr. 2016.

[5] J. Luszcz, High Frequency Conducted Emission in AC Motor Drives Fed By Frequency Converters: Sources and Propagation Paths. John Wiley & Sons, 2018.

[6] D. Drozhzhin and G. Griepentrog, "Simulation of Conducted Noise of an AC Drive by Means of Mixed Mode 6-Port Networks," In 2018 International Symposium on Electromagnetic Compatibility (EMC EUROPE), pp. 1-6, Aug. 2018.

[7] J. Xue and F. Wang, "Mixed-mode EMI noise in three-phase DC-fed PWM motor drive system," in 2013 IEEE Energy Conversion Congress and Exposition, pp. 4312–4317, Sep. 2013.